Prostaglandin E$_2$ Production and T Cell Function in Mouse Adenovirus Type 1 Infection following Allogeneic Bone Marrow Transplantation

Mary K. McCarthy[1¤], Megan C. Procario[2], Carol A. Wilke[3], Bethany B. Moore[1,3], Jason B. Weinberg[1,2]*

1 Department of Microbiology and Immunology, University of Michigan, Ann Arbor, Michigan, United States of America, 2 Department of Pediatrics and Communicable Diseases, Division of Infectious Diseases, University of Michigan, Ann Arbor, Michigan, United States of America, 3 Department of Internal Medicine, Division of Pulmonary and Critical Care Medicine, University of Michigan, Ann Arbor, Michigan, United States of America

¤ Current address: Department of Immunology and Microbiology, University of Colorado School of Medicine, Aurora, Colorado, United States of America
* jbwein@umich.edu

Abstract

Adenovirus infections are important complications of bone marrow transplantation (BMT). We demonstrate delayed clearance of mouse adenovirus type 1 (MAV-1) from lungs of mice following allogeneic BMT. Virus-induced prostaglandin E$_2$ (PGE$_2$) production was greater in BMT mice than in untransplanted controls, but BMT using PGE$_2$-deficient donors or recipients failed to improve viral clearance, and treatment of untransplanted mice with the PGE$_2$ analog misoprostol did not affect virus clearance. Lymphocyte recruitment to the lungs was not significantly affected by BMT. Intracellular cytokine staining of lung lymphocytes demonstrated impaired production of INF-γ and granzyme B by cells from BMT mice, and production of IFN-γ, IL-2, IL-4, and IL-17 following ex vivo stimulation was impaired in lymphocytes obtained from lungs of BMT mice. Viral clearance was not delayed in untransplanted INF-γ-deficient mice, suggesting that delayed viral clearance in BMT mice was not a direct consequence of impaired IFN-γ production. However, lung viral loads were higher in untransplanted CD8-deficient mice than in controls, suggesting that delayed MAV-1 clearance in BMT mice is due to defective CD8 T cell function. We did not detect significant induction of IFN-β expression in lungs of BMT mice or untransplanted controls, and viral clearance was not delayed in untransplanted type I IFN-unresponsive mice. We conclude that PGE$_2$ overproduction in BMT mice is not directly responsible for delayed viral clearance. PGE$_2$-independent effects on CD8 T cell function likely contribute to the inability of BMT mice to clear MAV-1 from the lungs.

Introduction

Viral infection is an important complication in both allogeneic and autologous bone marrow transplantation (BMT) [1–3]. Human adenoviruses (HAdVs) cause considerable morbidity and mortality in BMT patients [4–6]. Depending on the assay used, HAdVs have been detected in up to 29% of BMT patients during weekly surveillance screening [7,8]. Disease rates as high as 6.5% have been reported, with mortality rates of greater than 50% in BMT patients with HAdV disease in some studies [8,9]. Pediatric patients are at a higher risk for HAdV disease [6,10], likely due to higher infection rates in this population and a relative lack of HAdV species cross-reactive T and B cell responses compared to adults, in whom some HAdV-specific immunity has been established [11]. Severe graft-versus-host disease (GVHD) [12], T-cell-depleted grafts, and leukopenia [13] are additional risk factors for HAdV infection following BMT.

Profound defects in both innate and adaptive immune function are found following BMT [reviewed in [14]]. Both syngeneic and allogeneic BMT mice display defective control of viral replication in a mouse model of respiratory virus infection using murine gammaherpesvirus-68 (γHV-68) [14]. Levels of prostaglandin E_2 (PGE_2), a lipid mediator of immune function, are elevated in BMT patients [15,16] and in mouse models of BMT [17–19]. PGE_2 can be immuno-suppressive *in vitro*, inhibiting production of the Th1 cytokines IFN-γ and IL-12 [20,21]. Alveolar macrophage and neutrophil phagocytosis and bacterial killing are also inhibited by PGE_2 [22,23]. PGE_2 contributes to the suppression of lymphocyte function observed in human BMT patients [15]. Exaggerated PGE_2 production and increased susceptibility to *Pseudomonas aeruginosa* and *Staphylococcus aureus* infection occur in syngeneic BMT mice [17–19]. Such mice are unable to effectively control bacterial infections in the lung, and this is directly linked to the immunosuppressive effects of PGE_2 on macrophage and neutrophil function.

In vivo studies of HAdV pathogenesis are limited by the strict species-specificities of the adenoviruses. Inoculation of mice with HAdV does not result in a fully permissive infection [24,25] and therefore does not allow for a complete assessment of host inflammatory responses to adenovirus infection. In contrast, infection of mice with mouse adenovirus type 1 (MAV-1, also known as MAdV-1) serves as an excellent animal model system for studying adenovirus pathogenesis. MAV-1 virions have a morphology that resembles that of HAdV virions [26], and its genomic organization and the majority of its gene products are similar to HAdV counterparts [27–33]. We have worked extensively with MAV-1 as a model to study the pathogenesis of adenovirus respiratory infection [34–41]. MAV-1 targets the respiratory epithelium and replicates in the lungs following intranasal (i.n.) inoculation [35]. Acute MAV-1 respiratory infection causes pulmonary inflammation characterized by a patchy interstitial pneumonitis with scattered areas of hypercellularity around medium and large airways [35]. Interferon (IFN)-γ, interleukin (IL)-17 and other mediators such as prostaglandin E_2 are upregulated, and effector memory CD4 and CD8 T cells accumulate in the lungs of infected mice [35,37,40,41]. Neonatal mice are more susceptible than adult mice to MAV-1 respiratory infection, with higher lung viral loads, delayed virus clearance from the lungs, and immune responses that are blunted and delayed compared to those in adults [37].

Because HAdV infections are an important complication following allogeneic BMT, we examined pulmonary immunity to adenovirus infection following BMT using MAV-1. After i. n. MAV-1 infection, virus clearance from the lungs was significantly delayed in mice that received allogeneic BMT compared to untransplanted control mice. Our data suggest that T cell function is impaired in BMT mice. Delayed virus clearance was not related to exaggerated PGE_2 production, because allogeneic BMT using PGE_2-deficient mice as donors or recipients failed to correct the defect in viral clearance.

Materials and Methods

Mice

All animal studies were approved by the University of Michigan Committee on Use and Care of Animals. BALB/c, C57BL/6, CD8$\alpha^{-/-}$ [B6.129S2-$Cd8a^{tm1Mak}$/J], IFN-$\gamma^{-/-}$ [B6.129S7-$Ifng^{tm1Ts}$/J], and IFNAR$^{-/-}$ [B6.129S2-$Ifnar1^{tm1Agt}$/Mmjax] mice (all knockouts backcrossed onto a C57BL/6 background) were obtained from the Jackson Laboratory (Bar Harbor, ME). Mice heterozygous for microsomal prostaglandin E synthase-1 (mPGES-1) on a DBA1lac/J background (mPGES-1$^{-/-}$ mice) [42] were originally obtained from Pfizer, Inc. (Groton, CT) and then backcrossed onto a C57BL/6 background. Homozygous mPGES-1$^{-/-}$ mice and homozygous wt mPGES-1$^{+/+}$ mice derived from the same heterozygous mPGES-1$^{+/-}$ parents were bred at the University of Michigan. Adult males were used in all experiments. All mice were maintained under specific pathogen-free conditions.

Bone Marrow Transplantation

BMT was performed as previously described [14,17]. Recipient C57BL/6 mice received 1350 rad of total body irradiation using a ^{137}Cs irradiator, delivered in two doses 3 hours apart. In experiments in which C57BL/6 mice were used as donors in the allogeneic transplant, recipient BALB/c mice received 1000 rad of total body irradiation delivered in two doses 3 hours apart. Bone marrow cells (5 x 10^6) harvested from donor mice were injected into the tail vein of irradiated recipient mice. Mice were given acidified water (pH 3.3) for the first 3 weeks after BMT. Total hematopoietic cell numbers are fully reconstituted in the lung and spleen at 5 weeks post-BMT [14,43]. All infections were carried out 5–6 weeks following BMT. To confirm reconstitution of the lung and spleen in allogeneic BMT mice with donor-derived cells, alveolar macrophages (AM) and splenocytes were harvested from mice at 5 weeks post-BMT. The percentage of cells that were of donor or recipient origin was determined by flow cytometry using antibodies specific for H-2D^b (C57BL/6) and H-2D^d (BALB/c).

Virus and Infections

MAV-1 was grown and passaged in NIH 3T6 fibroblasts, and titers of viral stocks were determined by plaque assay on 3T6 cells as previously described [44]. Adult mice were anesthetized with ketamine and xylazine and infected i.n. with 10^5 plaque forming units of MAV-1 in 40 µl of sterile phosphate-buffered saline (PBS). Control mice were mock infected i.n. with conditioned media at an equivalent dilution in sterile PBS. Mice were euthanized by pentobarbital overdose at the indicated time points. Lungs were harvested, snap frozen in dry ice, and stored at -80°C until processed further.

Misoprostol treatment

Mice were injected intraperitoneally (i.p.) with 20 µg misoprostol once daily starting on the day of infection, a dosing regimen adapted from [45,46]. Control mice were injected i.p. with an equivalent volume of vehicle (DMSO).

Isolation of DNA and RNA

DNA was extracted from the middle lobe of the right lung using the DNeasy$^®$ Tissue Kit (Qiagen Inc.). Total RNA was extracted from lungs using TRIzol$^®$ (Invitrogen) as previously described [39].

Table 1. Primers and probes used for real-time PCR analysis.

Target	Oligonucleotide	Sequence (5′ to 3′)
MAV-1 E1A	Forward primer	GCACTCCATGGCAGGATTCT
	Reverse primer	GGTCGAAGCAGACGGTTCTTC
	Probe	TACTGCCACTTCTGC
IFN-β	Forward primer	AGCTCCAAGAAAGGACGAACAT
	Reverse primer	GCCCTGTAGGTGAGGTTGATCT
GAPDH	Forward primer	TGCACCACCAACTGCTTAG
	Reverse primer	GGATGCAGGGATGATGTTC

Analysis of Viral Loads

MAV-1 viral loads were measured in organs using quantitative real-time polymerase chain reaction (qPCR) as previously described [37,39]. Primers and probe used to detect a 59-bp region of the MAV-1 E1A gene are detailed in Table 1. Five µl of extracted DNA were added to reactions containing TaqMan II Universal PCR Mix with UNG (Applied Biosystems), forward and reverse primers (each at 200 nM final concentration), and probe (40 nM final concentration) in a 25 µl reaction volume. Analysis on an ABI Prism 7300 machine (Applied Biosystems) consisted of 40 cycles of 15 s at 90°C and 60 s at 60°C. Standard curves generated using known amounts of plasmid containing the MAV-1 EIA gene were used to convert cycle threshold values for experimental samples to copy numbers of EIA DNA. Results were standardized to the nanogram (ng) amount of input DNA. Each sample was assayed in triplicate. The limit of detection of this assay is typically between 10^1 and 10^2 copies of MAV-1 genome per 100 ng input DNA.

Analysis of Host Gene Expression

Cytokine gene expression was quantified using reverse transcriptase (RT)-qPCR. First, 2.5 µg of RNA were reverse transcribed using MMLV reverse transcriptase (Invitrogen) in 20 µl reactions according to the manufacturer's instructions. Water was added to the cDNA product to bring the total volume to 50 µl. Primers used to detect IFN-γ, granzyme B (GzmB), and IFN-β (PrimerBankID 7305123a1 [47]) are described in Table 1. For these measurements, 5 µl of cDNA were added to reactions containing Power SYBR Green PCR Mix (Applied Biosystems) and forward and reverse primers (each at 200 nM final concentration) in a 25 µl reaction volume. When SYBR green was used to quantify cytokine gene expression, separate reactions were prepared with primers for mouse GAPDH (Table 1, used at 200 nM each). In all cases, RT-qPCR analysis consisted of 40 cycles of 15 s at 90°C and 60 s at 60°C. Quantification of target gene mRNA was normalized to GAPDH and expressed in arbitrary units as $2^{-\Delta Ct}$, where Ct is the threshold cycle and $\Delta Ct = Ct(target) - Ct(GAPDH)$.

Analysis of PGE$_2$ Concentration in Bronchoalveolar Lavage Fluid

Mice were euthanized via pentobarbital overdose at the indicated time points. Lungs were lavaged three times with the same aliquot of 1 mL sterile PBS containing protease inhibitor (complete, Mini, EDTA-free tablets; Roche Applied Science). Cells in bronchoalveolar lavage fluid (BALF) were pelleted by centrifugation and supernatant was stored at -80°C until assayed. PGE$_2$ concentration in BALF was determined using a PGE$_2$ ELISA Kit (Enzo Life Sciences) according to the manufacturer's protocol.

Isolation of Cells from Lungs

In some experiments, left lungs were excised and cut into small pieces before digestion for 30 min at 37°C in a 1 mg/ml solution of collagenase A (Sigma). The digested tissue was then pushed through a syringe attached to a 1.5-in 22-gauge needle and pelleted at 3,000 rpm (402 x g) for 5 min. After lysis of red blood cells in 1X lysing buffer (BD PharMingen) for 3 min, tissue debris was removed by a brief spin (~5 to 10 s) at 1,000 rpm (45 x g). The remaining cells were pelleted at 1,200 rpm (64 x g) for 6 min prior to staining.

Intracellular Cytokine Staining

Cells isolated from lungs were plated at 10^6 cells/ml and stimulated with 50 ng/ml PMA and 1.5 μM ionomycin (Calbiochem) for 5 h at 37°C. Monensin (Sigma) was added at 3 μM for the last 3 hours of culture. Cells were preincubated with anti-FcγR mAb 2.4G2 to block nonspecific binding before they were stained with the following PE-Cy7-, APC-H7, and V450-conjugated antibodies: CD4 (RM4-5), CD8 (53–6.7), and TCR-β (H57-597) (BD Biosciences). Cells were then fixed in 4% paraformaldehyde for 10 min at room temperature, and permeabilized with 0.2% saponin (Sigma). Finally, cells were stained with FITC- and AF-647-labeled IFN-γ (XMG1.2) and GzmB (GB11) antibodies (BD Biosciences) and analyzed by flow cytometry. Events were acquired on a FACSCanto (BD) flow cytometer, and data were analyzed with FlowJo software (Tree Star). Cells were classified as CD4$^+$ T cells (TCRβ$^+$CD4$^+$) and CD8$^+$ T cells (TCRβ$^+$CD8$^+$).

Lymphocyte Stimulation

Lymphocytes were seeded at a concentration of 3 x 10^5 cells/well in 96-well plates coated with anti-CD3 antibody (BioLegend, 5 μg/ml) and incubated for 24 h. Supernatants were then collected for ELISA. Cytokine protein concentrations in supernatant were determined by ELISA (Duoset Kits, R&D Systems) according to the manufacturer's protocol.

Histology

Lungs were harvested from a subset of mice and fixed in 10% formalin. Prior to fixation, lungs were gently inflated with PBS via the trachea to maintain lung architecture. After fixation, organs were embedded in paraffin and 5 μm sections were obtained for histopathology. Sections were stained with hematoxylin and eosin to evaluate cellular infiltrates. All sectioning and staining was performed by the University of Michigan Comprehensive Cancer Center Research Histology and Immunoperoxidase Laboratory. Slides were viewed through a DM750 microscope (Leica Microsystems). Digital images were obtained with an ICC50 HD digital imaging system (Leica Microsystems) using Leica Acquisition Suite software (Leica Microsystems). Final images were assembled using Adobe Illustrator (Adobe Systems). To quantify cellular inflammation in the lungs, slides were examined in a blinded fashion to determine a pathology index as previously described [34,37].

Statistics

Analysis of data for statistical significance was conducted using Prism 6 for Macintosh (GraphPad Software, Incorporated). Log transformed values for viral load data were used for statistical comparisons. Differences between groups at multiple time points were analyzed using two-way analysis of variance (ANOVA) followed by Bonferroni's multiple comparison tests. Differences between multiple groups at a single time point were analyzed using one-way ANOVA followed by Bonferroni's or Tukey's multiple comparison tests. Comparisons between two groups at a

single time point were made using the Mann-Whitney rank sum test. Comparisons made between samples from the same mouse treated in two different ways were made using Wilcoxon matched pairs signed rank test. P values less than 0.05 were considered statistically significant.

Results

Delayed Viral Clearance from Lungs after Allogeneic BMT

To determine whether mice are more susceptible to MAV-1 infection following BMT, we first infected untransplanted C57BL/6 mice and syngeneic BMT mice (C57BL/6 donor and recipient) with MAV-1 at 5 weeks post-BMT, when numbers of hematopoietic cells are fully reconstituted [43]. We assessed viral loads in the lung at times corresponding to the peak of viral replication (7 dpi) and clearance of virus from the lungs (14 and 21 dpi). Viral loads were similar in syngeneic BMT mice and untransplanted controls at all times (Fig 1A). To determine whether mice are more susceptible following allogeneic BMT, we infected untransplanted control (BALB/c and C57BL/6) and allogeneic BMT (BALB/c donor, C57BL/6 recipient) mice with MAV-1 at 5 weeks post-BMT. Peak lung viral loads at 7 dpi were significantly higher in allogeneic BMT mice than in C57BL/6 controls at 7 dpi, but this difference was very small (Fig 1B). Viral loads were substantially lower in control mice at 14 and 21 dpi, as virus was cleared from the lungs. However, lung viral loads in allogeneic BMT mice did not substantially
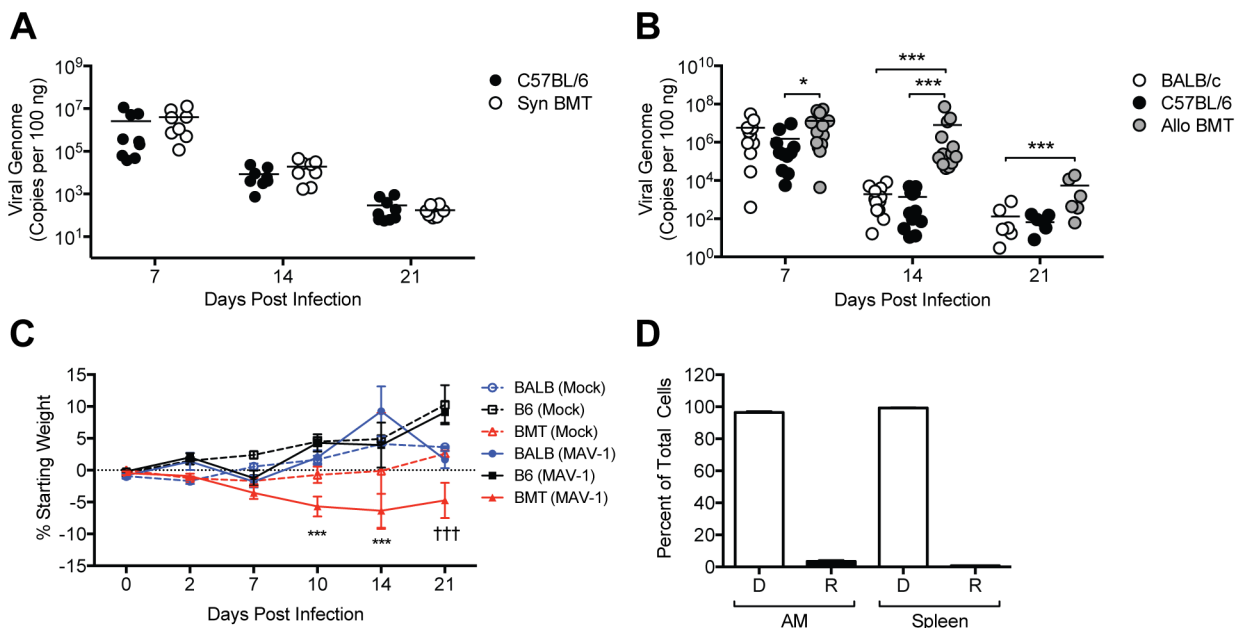

Fig 1. Delayed viral clearance from lungs of mice after allogeneic BMT. A) Syngeneic BMT mice (C57BL/6 donor and recipient) and untransplanted BALB/c and C57BL/6 controls were infected i.n. with MAV-1 at 5 weeks post BMT. DNA was extracted from lungs harvested at the indicated time points. qPCR was used to quantify MAV-1 genome copies in lung DNA. DNA viral loads are expressed as copies of MAV-1 genome per 100 ng of input DNA. B) Allogeneic BMT mice (BALB/c donor, C57BL/6 recipient) and untransplanted BALB/c and C57BL/6 controls were infected i.n. with MAV-1 and lung viral loads were quantified as above. In A and B, individual circles represent values for individual mice (n = 6 to 14 per group per time point) and horizontal bars represent means for each group. Statistical comparisons were made using two-way ANOVA followed by Bonferroni's multiple comparison tests. ***P<0.001, *P<0.05. C) Weight change was assessed in mock infected and infected allogeneic BMT mice and untransplanted controls (n = 3 to 14 per group, except n = 2 for mock infected B6 mice at 21 dpi). Weight gain or loss is expressed as the percentage of starting weight. ***P<0.001 comparing infected BMT mice to infected C57BL/6 and BALB/c controls; †††P<0.001 comparing infected BMT mice to infected C57BL/6 controls. D) In a separate allogeneic BMT experiment (BALB/c donor, C57BL/6 recipient), alveolar macrophages (AM) and splenocytes were harvested from uninfected mice at 5 weeks post-BMT. The percentage of cells that were of donor (D) or recipient (R) origin was determined by flow cytometry using antibodies specific for H-2D^b (C57BL/6) and H-2D^d (BALB/c). Combined data from n = 3 mice per group are presented as means ± S.E.M.

doi:10.1371/journal.pone.0139235.g001

decrease from 7 to 14 dpi, and they were significantly greater in allogeneic BMT mice than in control mice at 14 dpi. Lung viral loads in allogeneic BMT mice had decreased by 21 dpi, but they were still significantly greater than those in control mice.

Mock-infected untransplanted control mice, and mock infected BMT mice did not lose weight over the 21-day time course (Fig 1C), suggesting that GVHD was not present in the allogeneic BMT mice. MAV-1 infection did not induce weight loss in untransplanted control mice. In contrast, MAV-1 infection of BMT mice caused significant weight loss that was sustained over the 21-day time course. Reconstitution of the lung and spleen in allogeneic BMT mice with donor-derived cells was confirmed in a representative experiment by staining isolated alveolar macrophages and splenocytes with antibodies specific for H-2D^b (C57BL/6) and H-2D^d (BALB/c) (Fig 1D). These data indicate that peak viral replication was equivalent in control and allogeneic BMT mice, but viral clearance from the lungs was delayed and infection-induced weight loss was exacerbated in allogeneic BMT mice. Because delayed virus clearance was not present in syngeneic BMT mice, subsequent studies were performed in allogeneic BMT mice.

MAV-1-Induced Pulmonary Inflammation is Delayed in Allogeneic BMT

MAV-1 respiratory infection causes pulmonary inflammation characterized by scattered areas of hypercellularity around medium and large airways along with patchy interstitial pneumonitis comprised of a predominantly mononuclear infiltrate and thickened alveolar walls [35,37]. To determine whether delayed virus clearance and enhanced weight loss was associated with altered MAV-1-induced pulmonary inflammation in BMT mice, we evaluated the histological appearance of lungs from mock infected and infected BMT mice and untransplanted controls. Minimal inflammation was present in untransplanted BALB/c and C57BL/6 controls or BMT mice prior to infection (Fig 2A–2C) or in corresponding mock-infected groups at any time post infection (data not shown). Substantial peribronchial and interstitial cellular inflammation was present in BALB/c and C57BL/6 mice at 7 dpi (Fig 2D and 2E), but minimal inflammation was present in BMT mice at 7 dpi (Fig 2F). At 14 dpi, the degree of pulmonary inflammation was similar in lungs of BALB/c, C57BL/6, and BMT mice (Fig 2G–2I). Cellular inflammation had decreased but was still present at 21 dpi in BALB/c, C57BL/6, and BMT mice (Fig 2J–2L). We used a pathology index scoring system to quantify pulmonary inflammation at each time point (Fig 2M). Pathology scores were significantly less in infected BMT mice than in infected BALB/c or C57BL/6 mice at 7 dpi. There were no statistically significant differences in pathology scores in infected BALB/c, C57BL/6, or BMT mice at 14 or 21 dpi.

PGE$_2$ is Overproduced in Allogeneic BMT Infected with MAV-1

We previously demonstrated exaggerated PGE$_2$ production and susceptibility to bacterial infections in syngeneic BMT mice [17,18]. This increased susceptibility is linked to exaggerated PGE$_2$ production in BMT mice and to the immunosuppressive effects of PGE$_2$ on macrophages and neutrophils. To determine whether allogeneic BMT has a similar effect on PGE$_2$ production and MAV-1 pathogenesis, we measured PGE$_2$ concentrations in BALF before and after infection of allogeneic BMT mice. Prior to infection (5 weeks post-BMT), BALF PGE$_2$ concentrations were somewhat higher in BMT mice than in untransplanted BALB/c and C57BL/6 controls, although this difference was not statistically significant (Fig 3). After infection, PGE$_2$ concentrations increased modestly in both untransplanted control groups. In contrast, after infection of BMT mice, BALF PGE$_2$ concentrations increased dramatically, and PGE$_2$ production was significantly greater in BMT mice than either control group at 14 and 21 dpi.
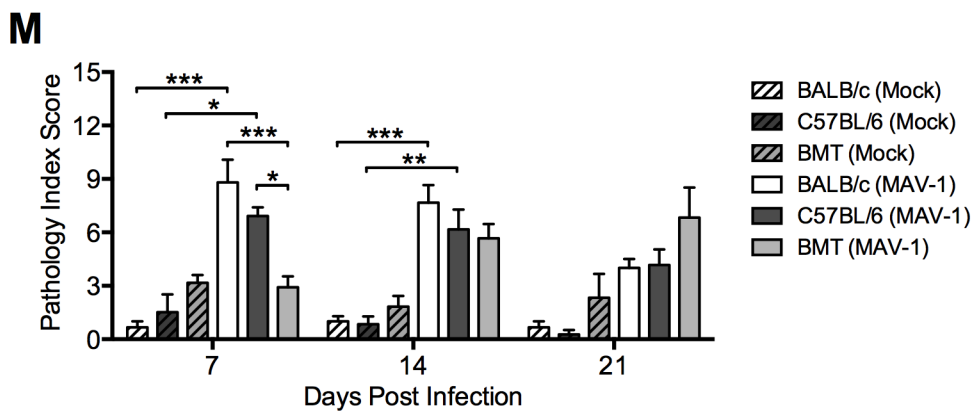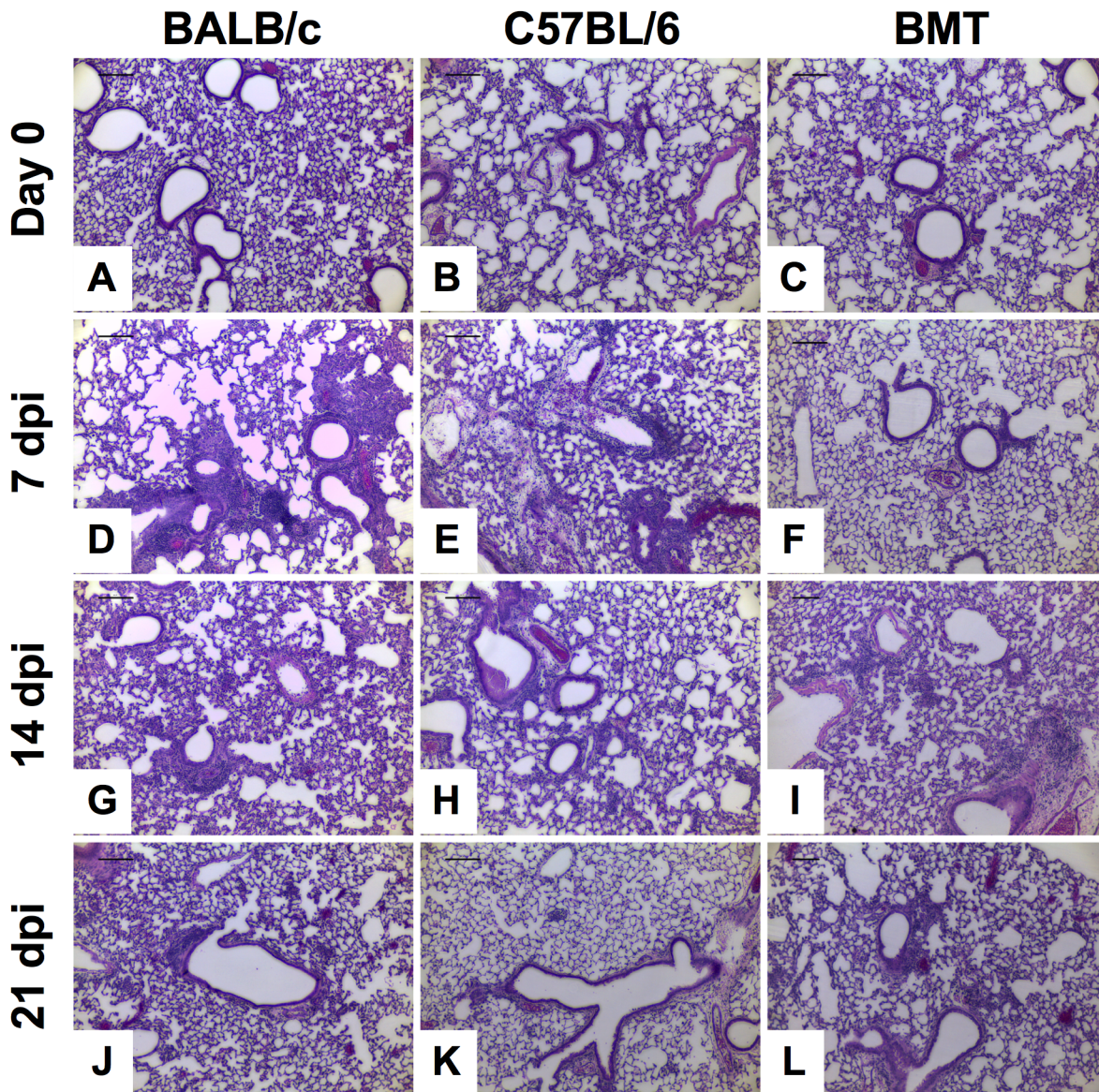
Fig 2. Virus-induced pulmonary inflammation in BMT mice. Allogeneic BMT mice (BALB/c donor, C57BL/6 recipient) and untransplanted BALB/c and C57BL/6 mice were infected i.n. with MAV-1 or mock infected at 5 weeks post BMT. Lungs were harvested and hematoxylin-and-eosin-stained sections were

prepared from paraffin-embedded specimens. Representative images are shown from mice before infection (A-C) and from infected mice at the indicated time points (D-L). Scale bars, 100 µm. M) Pathology index scores were generated to quantify cellular inflammation in the lungs of mock-infected and infected mice. Data from 2 to 3 mock-infected mice and 3 to 6 infected mice per group are presented as means and standard errors of the means at each time point. Statistical comparisons were made using two-way ANOVA followed by Bonferroni's multiple comparison tests. *$P<0.05$, **$P<0.01$, and ***$P<0.001$.

doi:10.1371/journal.pone.0139235.g002

PGE$_2$ Overproduction Does Not Contribute to Delayed Viral Clearance in BMT Mice

To determine whether PGE$_2$ overproduction directly contributes to delayed viral clearance in BMT mice, we performed allogeneic BMT using mPGES-1$^{-/-}$ mice as donors or recipients. mPGES-1 is the terminal synthase responsible for the majority of the conversion of the intermediate PGH$_2$ to PGE$_2$, so that mPGES-1-deficient mice on a C57BL/6 background (indicated as mPGES-1$^{-/-}$/B6) are almost completely PGE$_2$-deficient [48,49]. We infected mice with MAV-1 at 5 weeks post-BMT and measured BALF PGE$_2$ at 14 dpi. Virus-induced PGE$_2$ was greater in allogeneic BMT mice (BALB/c donor, C57BL/6 recipient), than in untransplanted BALB/c and C57BL/6 control mice (Fig 4A), consistent with our previous observation (Fig 2). When BALB/c bone marrow was transferred into mPGES-1$^{-/-}$/B6 recipients, virus-induced PGE$_2$ concentrations were equivalent to those measured in C57BL/6 mice that received BALB/c bone marrow. This suggests that hematopoietic cells from BALB/c donors (which are not PGE$_2$-deficient) were the major source of PGE$_2$ in infected BMT mice.

To create a situation in which the immune cell compartment was deficient in PGE$_2$, we used C57BL/6 or mPGES-1$^{-/-}$/B6 mice as donors and BALB/c mice as recipients. Compared to BMT using BALB/c donors and C57BL/6 recipients, we observed significantly less virus-induced PGE$_2$ production at 14 dpi in BMT using C57BL/6 mice as donors and BALB/c mice as recipients (Fig 4A). When mPGES-1$^{-/-}$/B6 bone marrow was transferred into BALB/c mice, virus-induced PGE$_2$ production was equivalent to that of either untransplanted control group. The differences in PGE$_2$ production observed in BMT combinations using C57BL/6 mice and BALB/c mice as recipients may relate to differing amounts of irradiation received at the time of transplant (1350 rad for C57BL/6 versus 1000 rad for BALB/c) given the higher sensitivity of BALB/c mice to radiation [50]. Despite varying levels of PGE$_2$ production, all combinations of allogeneic BMT mice using PGE$_2$-deficient mice as donors or recipients had significantly higher lung viral loads at 14 dpi compared to either untransplanted control group (Fig 4B). In
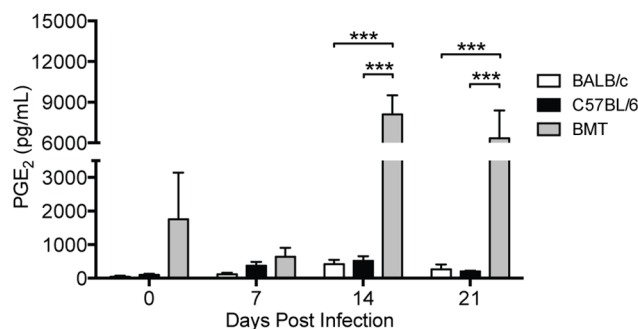

Fig 3. PGE$_2$ is overproduced in BMT mice. BMT mice (BALB/c donor, C57BL/6 recipient) and untransplanted BALB/c and C57BL/6 controls were infected i.n. with MAV-1 or mock infected with conditioned media. ELISA was used to quantify PGE$_2$ concentrations in BALF at the indicated time points. Combined data from n = 3–4 mice per group are presented as means ± S.E.M. Statistical comparisons were made using two-way ANOVA followed by Bonferroni's multiple comparison tests. ***$P<0.001$.
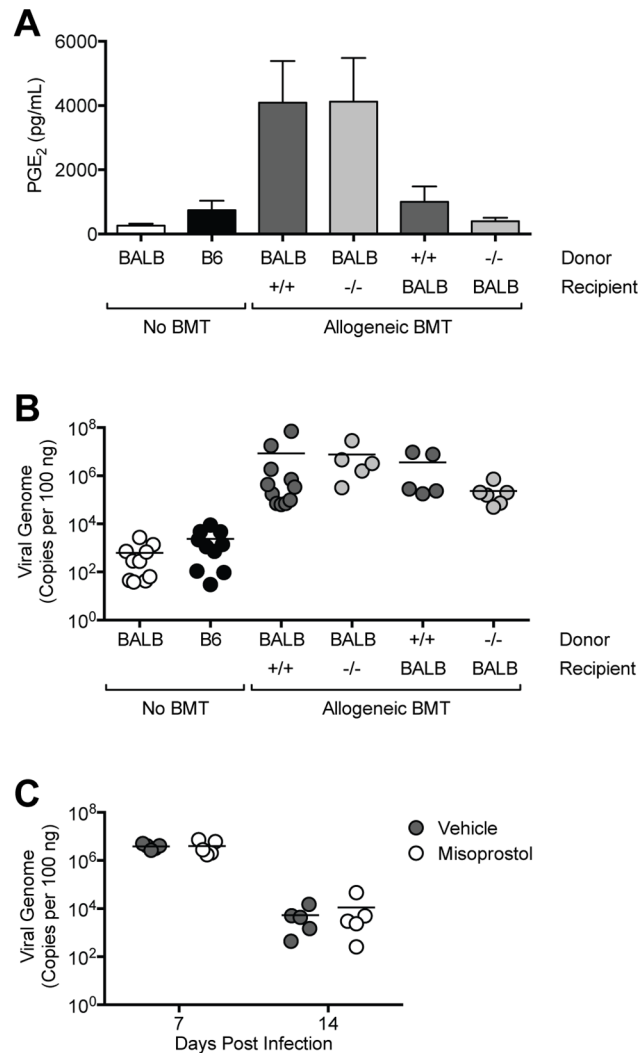
doi:10.1371/journal.pone.0139235.g003

Fig 4. Restoration of normal PGE$_2$ levels fails to correct delayed viral clearance in BMT mice.
Allogeneic BMT was performed using mPGES-1$^{+/+}$ (+/+) or mPGES-1$^{-/-}$ (-/-) mice on a C57BL/6 background with BALB/c mice in the indicated combinations. BMT mice and untransplanted BALB/c (BALB) and C57BL/6 (B6) controls were infected i.n. with MAV-1 or mock infected with conditioned media. A) ELISA was used to quantify PGE$_2$ concentrations in BALF at the indicated time points. Combined data from n = 5–15 mice per group are presented as means ± S.E.M. B) DNA was extracted from lungs harvested at 14 dpi. qPCR was used to quantify MAV-1 genome copies in lung DNA. DNA viral loads are expressed as copies of MAV-1 genome per 100 ng of input DNA. Individual circles represent values for individual mice and horizontal bars represent means for each group. C) C57BL/6 mice were infected i.n. with MAV-1 and treated once daily with 20 μg misoprostol or vehicle (DMSO). DNA was extracted from lungs harvested at the indicated time points. qPCR was used to quantify MAV-1 genome copies in lung DNA. DNA viral loads are expressed as copies of MAV-1 genome per 100 ng of input DNA. Individual circles represent values for individual mice and horizontal bars represent means for each group.

doi:10.1371/journal.pone.0139235.g004

addition, we observed no significant differences in virus-induced pulmonary inflammation in all combinations of allogeneic BMT using PGE$_2$-deficient mice (data not shown).

To examine the effects of excess PGE$_2$ on MAV-1 infection in the absence of other potential effects caused by BMT, we treated untransplanted C57BL/6 mice with misoprostol, a PGE$_2$ analog, beginning on the day of infection. Misoprostol treatment did not affect peak viral replication at 7 dpi or viral clearance from the lungs at 14 dpi (Fig 4C). Thus, although PGE$_2$ was

produced in excess in allogeneic BMT mice following MAV-1 infection, our data collectively indicate that PGE$_2$ overproduction did not directly contribute to delayed viral clearance in allogeneic BMT mice.

T Cell Function is Impaired During MAV-1 Infection of Allogeneic BMT Mice

Because delayed virus clearance in BMT mice was not a consequence of PGE$_2$ overproduction, we considered other aspects of immune function that could affect MAV-1 clearance during BMT. Impaired CD8 T cell immunity contributes to increased severity of disease caused by Sendai virus in allogeneic BMT mice [51]. We therefore hypothesized that the inability of allogeneic BMT mice to efficiently clear virus from the lungs could be due to impaired T cell recruitment or function during MAV-1 infection. To assess overall CD4 and CD8 T cell recruitment and function, we isolated lung lymphocytes from untransplanted BALB/c and allogeneic BMT mice (in which hematopoietic cells were derived from the BALB/c donor strain) at 7 dpi and used flow cytometry to characterize T cell subsets. There were fewer TCRβ$^+$CD4$^+$ T cells in the lungs of BMT mice compared to BALB/c mice both before and after infection, although these differences were not statistically significant (Fig 5A). BALB/c and BMT mice had equivalent numbers of TCRβ$^+$CD8$^+$ T cells in the lungs after infection (Fig 5B). We performed intracellular cytokine staining to evaluate T cell cytokine production at 7 dpi. In untransplanted BALB/c mice, there were more CD4 and CD8 T cells producing IFN-γ (Fig 5C) or GzmB (Fig 5D) after MAV-1 infection. However, numbers of IFN-γ$^+$ and GzmB$^+$ CD4 and CD8 T cells were significantly less in infected BMT mice. Because there were no significant differences between the numbers of CD8 and CD4 T cells in lungs of BMT mice compared to controls, but the numbers of IFN-γ-producing and GzmB-producing cells were substantially less in BMT mice, our data suggest that T cell function, but not recruitment, was impaired in allogeneic BMT mice infected by MAV-1.

CD8 T Cells Contribute to MAV-1 Clearance in an IFN-γ-Independent Manner

To further address T cell function in allogeneic BMT mice, we isolated lung lymphocytes from BMT mice and untransplanted BALB/c controls at 7 dpi, restimulated the cells overnight with anti-CD3 antibody, and measured IFN-γ concentrations in supernatant following restimulation. Cells isolated from infected, untransplanted BALB/c mice produced significantly more IFN-γ upon restimulation than cells isolated from mock infected BALB/c mice (Fig 6A). To determine the extent to which deficient IFN-γ responses in BMT mice contributed to delayed clearance of MAV-1, we infected untransplanted IFN-γ$^{+/+}$ and IFN-γ$^{-/-}$ mice and measured lung viral loads at 14 dpi. Viral loads were equivalent in IFN-γ$^{+/+}$ and IFN-γ$^{-/-}$ mice (Fig 6B), suggesting that decreased IFN-γ production by lymphocytes in BMT mice did not play a significant role in delayed viral clearance. Similarly, we have shown that IFN-γ deficiency on a BALB/c background leads to only a modest (<1 log) increase in MAV-1 viral loads at 14 dpi [37].

We also observed that production of IL-2 (Fig 7A) along with IL-4 and IL-17 (S1 Fig) by lung lymphocytes isolated from BMT mice was impaired compared to production by lung lymphocytes isolated from untransplanted BALB/c controls. We have previously demonstrated that MAV-1 lung viral loads are not affected by IL-17 deficiency [40], so effects of BMT on IL-17 production are unlikely to have contributed to delayed viral clearance in BMT mice. However, because IL-2 makes critical contributions to CD8 T cell proliferation, differentiation, and effector function [52], this further suggested that CD8 T cell function was impaired in BMT
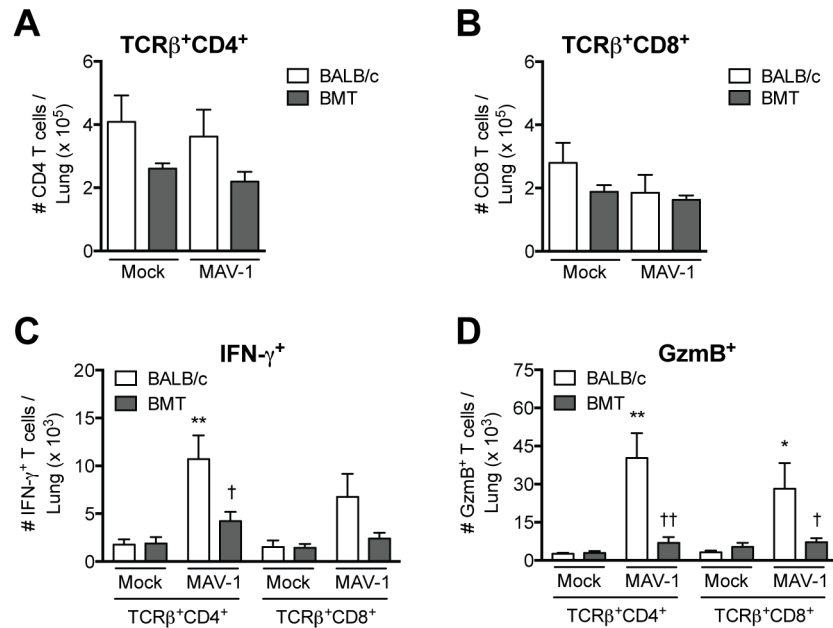
Fig 5. T cells in lungs of BMT mice. BMT mice (BALB/c donor, C57BL/6 recipient) and untransplanted BALB/c and C57BL/6 controls were infected i.n. with MAV-1 or mock infected with conditioned media. Lung leukocytes isolated at 7 dpi were stimulated with PMA/ionomycin and stained to quantify the number of A) TCRβ+CD4+ T cells, B) TCRβ+CD8+ T cells, C) IFN-γ+ T cells, and D) GzmB+ T cells per lung. Combined data from n = 3–4 mice per group are presented as means ± S.E.M. Statistical comparisons were made using one-way ANOVA followed by Bonferroni's multiple comparison tests. **$P<0.01$ and *$P<0.05$ comparing mock to MAV-1. ††$P<0.01$ and †$P<0.05$ comparing BALB/c to BMT mice.

doi:10.1371/journal.pone.0139235.g005

mice. To determine whether aspects of CD8 T cell function other than IFN-γ production were required for viral clearance, we infected CD8α+/+ and CD8α-/- mice with MAV-1 and measured lung viral loads at 14 dpi. Viral loads were significantly greater in CD8α-/- mice compared to CD8α+/+ mice ([Fig 7B]). These results indicate that CD8 T cells contribute to clearance
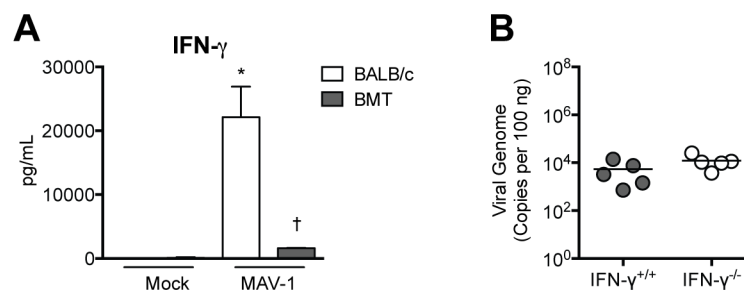

Fig 6. Impaired IFN-γ production in BMT mice. A) BMT mice (BALB/c donor, C57BL/6 recipient) and untransplanted BALB/c controls were infected i.n. with MAV-1 or mock infected with conditioned media, and lung leukocytes were isolated at 7 dpi. Lung leukocytes were stimulated overnight with anti-CD3 antibody and ELISA was used to measure IFN-γ concentrations in supernatants. Combined data from n = 3–8 mice per group are presented as means ± S.E.M. Statistical comparisons were made using one-way ANOVA followed by Tukey's multiple comparison tests. **$P<0.01$ and *$P<0.05$ comparing mock to MAV-1. ††$P<0.01$ and †$P<0.05$ comparing BALB/c to BMT mice. B) A) IFN-γ+/+ and IFN-γ-/- mice were infected i.n. with MAV-1. DNA was extracted from lungs harvested at 14 dpi. qPCR was used to quantify MAV-1 genome copies in lung DNA. DNA viral loads are expressed as copies of MAV-1 genome per 100 ng of input DNA. Individual circles represent values for individual mice and horizontal bars represent means for each group. Statistical comparisons were made using the Mann-Whitney test.

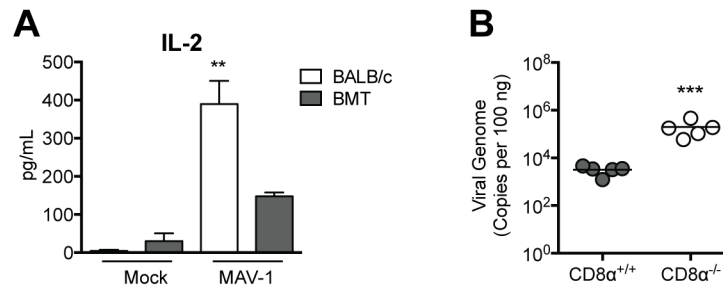doi:10.1371/journal.pone.0139235.g006

Fig 7. Delayed viral clearance in the absence of CD8 T cells. A) BMT mice (BALB/c donor, C57BL/6 recipient) and untransplanted BALB/c controls were infected i.n. with MAV-1 or mock infected with conditioned media, and lung leukocytes were isolated at 7 dpi. Lung leukocytes were stimulated overnight with anti-CD3 antibody and ELISA was used to measure IL-2 concentrations in supernatants. Combined data from n = 3–8 mice per group are presented as means ± S.E.M. Statistical comparisons were made using one-way ANOVA followed by Tukey's multiple comparison tests. **$P<0.01$ and *$P<0.05$ comparing mock to MAV-1. B) CD8$\alpha^{+/+}$ and CD8$\alpha^{-/-}$ mice were infected i.n. with MAV-1. DNA was extracted from lungs harvested at 14 dpi. qPCR was used to quantify MAV-1 genome copies in lung DNA. DNA viral loads are expressed as copies of MAV-1 genome per 100 ng of input DNA. Individual circles represent values for individual mice and horizontal bars represent means for each group. Statistical comparisons were made using the Mann-Whitney test. ***$P<0.001$.

of virus from the lung during MAV-1 infection, although not via production of IFN-γ. Taken together, these data suggest that CD8 T cell dysfunction contributed to delayed virus clearance in BMT mice.

Type I IFN Responses Do Not Contribute to Delayed Virus Clearance in BMT Mice

To determine whether allogeneic BMT modulated type I IFN responses in a way that could affect MAV-1 pathogenesis, we used RT-qPCR to quantify mRNA levels of IFN-β in the lungs of BMT mice and untransplanted controls (Fig 8A). IFN-β mRNA levels were slightly lower in BMT mice than in untransplanted controls prior to infection, but this difference was not statistically significant. There were no statistically significant differences in IFN-β mRNA levels between BMT mice and untransplanted controls at any time point (Fig 8A). In addition, we infected untransplanted mice deficient in type I IFN signaling (IFNAR$^{-/-}$ mice) and B6 controls and measured lung viral loads at 7 and 14 dpi (Fig 8B). Viral loads were equivalent in B6 and IFNAR$^{-/-}$ mice at each time point. Thus, our data indicate that type I IFN activity is not essential for control of MAV-1 replication or for clearance of virus from the lungs.

Discussion

HAdV infection is a potentially devastating complication in hematopoietic stem cell transplant (HSCT) patients, and there are no antiviral or immunomodulatory therapies that have consistently shown a benefit in HSCT patients with HAdV disease. We used MAV-1 to study the effects of BMT on host susceptibility to adenovirus infection. Mice that underwent allogeneic BMT displayed significant defects in clearance of MAV-1 from the lungs. This altered susceptibility in allogeneic BMT mice was independent of pharmacologic immunosuppression that is typically used in transplant recipients. It occurred at a time post-BMT at which significant GVHD, a risk factor for HAdV infection in some reports [12] was not present in the allogeneic BMT mice ([14] and data not shown). However, syngeneic BMT had no effect on clearance of MAV-1 from the lungs. Thus, allogeneic BMT itself was associated with intrinsic changes in host immune function that impaired control of MAV-1 infection in the lung.
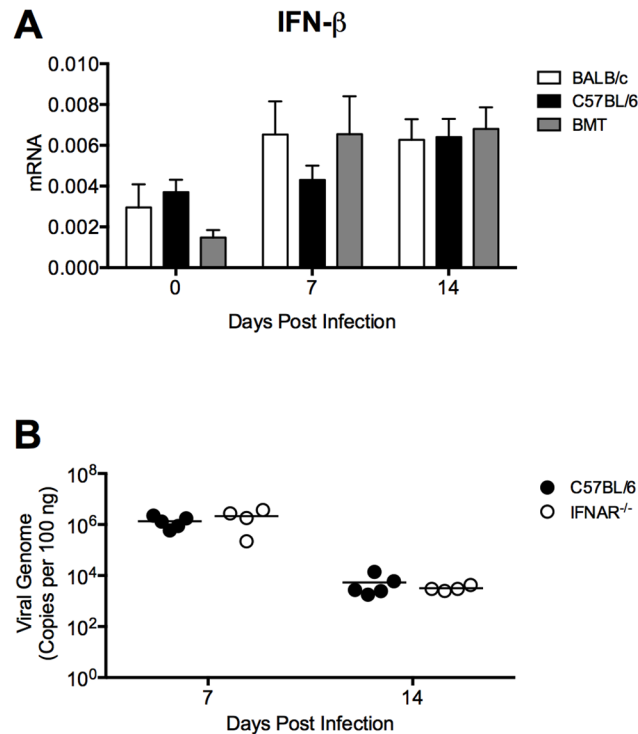
Fig 8. Type I IFN production in BMT mice. A) BMT mice (BALB/c donor, C57BL/6 recipient) and untransplanted BALB/c and C57BL/6 controls were infected i.n. with MAV-1, and lungs were harvested at the indicated time points. RT-qPCR was used to quantify IFN-β mRNA levels. Combined data from n = 7–8 mice per group (n = 3 per group at day 0) are presented as means ± S.E.M. Statistical comparisons were made using two-way ANOVA followed by Bonferroni's multiple comparison tests. B) Untransplanted C57BL/6 and IFNAR$^{-/-}$ mice were infected i.n. with MAV-1. DNA was extracted from lungs harvested at the indicated time points. qPCR was used to quantify MAV-1 genome copies in lung DNA. DNA viral loads are expressed as copies of MAV-1 genome per 100 ng of input DNA. Individual circles represent values for individual mice and horizontal bars represent means for each group. Statistical comparisons were made using two-way ANOVA followed by Bonferroni's multiple comparison tests.

doi:10.1371/journal.pone.0139235.g008

Concentrations of the immunomodulatory lipid mediator PGE$_2$ were dramatically higher in BALF from allogeneic BMT mice than in untransplanted controls after MAV-1 infection. However, allogeneic BMT using PGE$_2$-deficient mice as donors or recipients failed to correct the defect in viral clearance, and treatment of untransplanted mice with the PGE$_2$ analog misoprostol was not associated with increased lung viral loads. T cell recruitment to the lungs was not significantly affected by BMT, similar to our previous findings in syngeneic BMT mice [14]. BMT mice had significantly fewer IFN-γ-producing and GzmB-producing CD4 and CD8 T cells in the lungs compared to untransplanted controls, and cytokine production by restimulated T cells was substantially lower in T cells isolated from BMT mice compared to controls. Lung viral loads in untransplanted CD8-deficient mice were higher than in wt mice, suggesting that a defect in CD8 T cell function contributed to delayed MAV-1 clearance in BMT mice.

We previously demonstrated that acute MAV-1 infection increases PGE$_2$ production in the lungs of untransplanted C57BL/6 mice, but PGE$_2$ deficiency (in mPGES-1$^{-/-}$ mice) has little effect on the amount of viral replication in the lungs, clearance of virus from the lungs, or virus-induced lung inflammation [41]. In this study, we addressed the question of whether exaggerated virus-induced PGE$_2$ production in BMT, a scenario that is distinct from induction of PGE$_2$ production in an immunocompetent host, would affect MAV-1 pathogenesis. We detected dramatically increased PGE$_2$ in the airways following MAV-1 infection of allogeneic

BMT mice, similar to findings from other studies using mouse models of bacterial infection [17–19] or γHV-68 infection [53] following syngeneic BMT. PGE_2 suppresses the production of Th1 cytokines [20,21], an effect that is observed when local PGE_2 concentrations are greater than 1 nM [54]. Others have demonstrated PGE_2 inhibition of T cell proliferation in mixed lymphocyte reactions (MLR) [55]. PGE_2 inhibits T cell recruitment and delays the induction of virus-specific T cell responses in the lungs of influenza virus-infected mice [56]. We hypothesized that overproduction of PGE_2 in allogeneic BMT mice was responsible for suppression of T cell responses that normally clear virus from the lung. However, BMT using PGE_2-deficient mice as donors or recipients did not correct the defect in viral clearance. The amount of PGE_2 detected in those experiments varied based on donor and recipient background strain, most likely due to differences in the amount of irradiation used for BALB/c versus C57BL/6 recipients at the time of transplant. However, virus clearance was delayed in all transplanted mice despite the absence of increased PGE_2. In addition, untransplanted mice treated with the PGE_2 analog misoprostol cleared virus as efficiently as controls. Thus, while PGE_2 is overproduced after allogeneic BMT and suppresses T cell responses in other settings, our data suggest that PGE_2 overproduction does not contribute to delayed clearance of MAV-1 following allogeneic BMT.

While PGE_2 overproduction was apparently not the cause of T cell dysfunction, our data indicate that aberrant T cell function in allogeneic BMT mice is a potential explanation for delayed virus clearance. This is similar to findings in a recent study indicating that impaired clearance of Sendai virus in allogeneic BMT is due to T cell dysfunction [51]. In our study, $CD8\alpha^{-/-}$ mice had higher viral loads than $CD8\alpha^{+/+}$ mice at 14 dpi, suggesting that $CD8\alpha^{-/-}$ mice had a defect in clearance of virus from the lungs similar to that observed in allogeneic BMT mice. Although allogeneic BMT mice had significantly fewer IFN-γ-producing CD8 T cells and less IFN-γ production following lymphocyte restimulation, IFN-$γ^{-/-}$ mice cleared virus from the lungs as efficiently as IFN-$γ^{+/+}$ controls. Similarly, we have previously shown that IFN-γ makes only minor contributions to control of MAV-1 replication in another mouse strain background, BALB/c [37]. It is therefore unlikely that delayed virus clearance in allogeneic BMT mice was a direct consequence of BMT-associated changes in T cell IFN-γ production. Likewise, changes in type I IFN production are not likely to explain delayed virus clearance. Rather, delayed MAV-1 clearance from the lungs of BMT mice may be due to alterations in other aspects of cytotoxic T cell function (e.g. GzmB, perforin or Fas/FasL signaling), since MAV-1 clearance was similarly impaired in $CD8\alpha^{-/-}$ mice but not IFN-$γ^{-/-}$ mice. It is possible that CD8 T cell dysfunction in allogeneic BMT mice infected with MAV-1 was due to enhanced suppression via interactions between programmed death 1 and PD-1 ligand proteins, as is the case with Sendai virus infection in allogeneic BMT [51]. Future studies will systematically address which CD8 effector functions are most critical for clearance of MAV-1 as well as the specific mechanisms underlying T cell dysfunction post-BMT.

The difference between lung viral loads at 14 dpi in $CD8\alpha^{-/-}$ and $CD8\alpha^{+/+}$ mice (Fig 7B, approximately 2 log) was not as great as the difference between BMT mice and controls (Fig 1B, approximately 4 log). This suggests that impairment of other aspects of host immune function is likely to contribute to delayed clearance of MAV-1. The requirement for IFN-γ production to control viral clearance is pathogen-specific. While CD4 T cell-derived IFN-γ is important for clearance of lytic γHV-68 infection in BMT mice [14], our results suggest that IFN-γ is not required for clearance of MAV-1 from the lungs. Although contributions of CD4 T cells to clearance of MAV-1 from the lungs have yet to be fully defined, we previously demonstrated that lung viral loads are slightly higher in MHC class II-deficient mice at 7 dpi [41]. It is therefore possible that CD4 T cell dysfunction also contributes to delayed MAV-1 clearance in allogeneic BMT mice, but this is unlikely to be directly related to IFN-γ production by

CD4 T cells. Although it is possible that antigen presenting cell dysfunction may have contributed to some of the observed effects, we have previously demonstrated that antigen presenting cell function is intact in syngeneic BMT mice [14].

We conclude that allogeneic BMT is associated with PGE_2 overproduction, T cell dysfunction, and impaired clearance of MAV-1 from the lungs. However, excess PGE_2 does not directly contribute to the delayed virus clearance. It is possible that increased viral replication at late time points, resulting from delayed virus clearance in BMT mice due to T cell dysfunction, was actually the cause of exaggerated PGE_2 production instead of its indirect consequence. Our results emphasize the importance of immune dysfunction that is intrinsic to allogeneic BMT, distinct from effects of immunosuppressive medications used in transplant recipients. Our findings are similar to those in transplant recipients infected with HAdV. Immune recovery appears to play a significant role in HAdV infections post-transplantation. A number of studies have documented a positive correlation between lymphocyte count (both absolute lymphocyte count and CD4 count) and clearance of HAdV and survival [13,57,58]. In adult and pediatric HSCT patients, clearance of HAdV from peripheral blood is associated with the emergence of HAdV-specific CD4 and CD8 T cell responses [59]. Clearance of HAdV is also associated with an increase in titers of serotype-specific antibodies [57], indicating that both B and T cell function may be important for control of HAdV post-transplantion.

Ex vivo generation and adoptive transfer of virus-specific CD4 or CD8 T cells has been explored as immunotherapy for HSCT patients with disease caused by HAdV and other viruses. This strategy has been successfully used in transplant patients with Epstein Barr virus-induced lymphoproliferative disease [60–62] and with some success in pediatric transplant patients with HAdV viremia [63] or prophylactically to prevent HAdV disease [64]. A number of studies have demonstrated *ex vivo* generation of HAdV-specific cytotoxic CD4 and CD8 T cells, some of which were cross-reactive against multiple HAdV serotypes [65–70]. *Ex vivo* generation of single-culture T cells specific for HAdV and five other viruses has also been used as an approach to treat transplant patients infected with multiple viruses at the same time [71]. These studies show promise for the effective treatment of HAdV infections post-HSCT. The results of our work with MAV-1 in BMT expand our understanding of adenovirus pathogenesis in an immunocompromised host. Our model is well suited for future work to improve preventative and treatment strategies used for transplant recipients with disease caused by HAdV and other pathogens.

Supporting Information

S1 Dataset. Complete data for all experiments described in this manuscript are included in the file "BMT and MAV-1 Manuscript PLOS ONE Complete Data 081115.xlsx."
(XLSX)

S1 Fig. Impaired Cytokine production in BMT mice. BMT mice (BALB/c donor, C57BL/6 recipient) and untransplanted BALB/c controls were infected i.n. with MAV-1 or mock infected with conditioned media, and lung leukocytes were isolated at 7 dpi. Lung leukocytes were stimulated overnight with anti-CD3 antibody and ELISA was used to measure concentrations of A) IL-4 and B) IL-17 in supernatants. Combined data from n = 3–8 mice per group are presented as means ± S.E.M. Statistical comparisons were made using one-way ANOVA followed by Tukey's multiple comparison tests. $^{**}P<0.01$ comparing mock to MAV-1. $††P<0.01$ comparing BALB/c to BMT mice.
(TIFF)

Acknowledgments

The authors thank Racquel Domingo-Gonzalez and Tom Moore for help with analyzing reconstitution of the bone marrow chimeras by flow cytometry, Kathy Spindler and Mike Imperiale for helpful review of the manuscript, and Michael Watson for the use of the microscope and imaging system.

Author Contributions

Conceived and designed the experiments: MKM BBM JBW. Performed the experiments: MKM MCP CAW JBW. Analyzed the data: MKM MCP BBM JBW. Wrote the paper: MKM MCP BBM JBW.

References

1. Martin-Pena A, Aguilar-Guisado M, Espigado I, Parody R, Miguel Cisneros J (2011) Prospective study of infectious complications in allogeneic hematopoietic stem cell transplant recipients. Clin Transplant 25: 468–474. doi: 10.1111/j.1399-0012.2010.01286.x PMID: 20482561

2. Gil L, Styczynski J, Komarnicki M (2007) Infectious complication in 314 patients after high-dose therapy and autologous hematopoietic stem cell transplantation: risk factors analysis and outcome. Infection 35: 421–427. PMID: 17926001

3. Auner HW, Sill H, Mulabecirovic A, Linkesch W, Krause R (2002) Infectious complications after autologous hematopoietic stem cell transplantation: comparison of patients with acute myeloid leukemia, malignant lymphoma, and multiple myeloma. Ann Hematol 81: 374–377. PMID: 12185506

4. Walls T, Shankar AG, Shingadia D (2003) Adenovirus: an increasingly important pathogen in paediatric bone marrow transplant patients. Lancet Infect Dis 3: 79–86. PMID: 12560192

5. Kojaoghlanian T, Flomenberg P, Horwitz MS (2003) The impact of adenovirus infection on the immuno-compromised host. Rev Med Virol 13: 155–171. PMID: 12740831

6. Baldwin A, Kingman H, Darville M, Foot AB, Grier D, et al. (2000) Outcome and clinical course of 100 patients with adenovirus infection following bone marrow transplantation. Bone Marrow Transplant 26: 1333–1338. PMID: 11223974

7. Runde V, Ross S, Trenschel R, Lagemann E, Basu O, et al. (2001) Adenoviral infection after allogeneic stem cell transplantation (SCT): report on 130 patients from a single SCT unit involved in a prospective multi center surveillance study. Bone Marrow Transplant 28: 51–57. PMID: 11498744

8. Flomenberg P, Babbitt J, Drobyski WR, Ash RC, Carrigan DR, et al. (1994) Increasing incidence of adenovirus disease in bone marrow transplant recipients. J Infect Dis 169: 775–781. PMID: 8133091

9. Hierholzer JC (1992) Adenoviruses in the immunocompromised host. Clin Microbiol Rev 5: 262–274. PMID: 1323383

10. Howard DS, Phillips IG, Reece DE, Munn RK, Henslee-Downey J, et al. (1999) Adenovirus infections in hematopoietic stem cell transplant recipients. Clin Infect Dis 29: 1494–1501. PMID: 10585802

11. Leen AM, Bollard CM, Myers GD, Rooney CM (2006) Adenoviral infections in hematopoietic stem cell transplantation. Biol Blood Marrow Transplant 12: 243–251. PMID: 16503493

12. Shields AF, Hackman RC, Fife KH, Corey L, Meyers JD (1985) Adenovirus infections in patients undergoing bone-marrow transplantation. N Engl J Med 312: 529–533. PMID: 2982098

13. Chakrabarti S, Mautner V, Osman H, Collingham KE, Fegan CD, et al. (2002) Adenovirus infections following allogeneic stem cell transplantation: incidence and outcome in relation to graft manipulation, immunosuppression, and immune recovery. Blood 100: 1619–1627. PMID: 12176880

14. Coomes SM, Wilke CA, Moore TA, Moore BB (2010) Induction of TGF-beta 1, not regulatory T cells, impairs antiviral immunity in the lung following bone marrow transplant. J Immunol 184: 5130–5140. doi: 10.4049/jimmunol.0901871 PMID: 20348421

15. Klingemann HG, Tsoi MS, Storb R (1986) Inhibition of prostaglandin E2 restores defective lymphocyte proliferation and cell-mediated lympholysis in recipients after allogeneic marrow grafting. Blood 68: 102–107. PMID: 2941083

16. Cayeux SJ, Beverley PC, Schulz R, Dorken B (1993) Elevated plasma prostaglandin E2 levels found in 14 patients undergoing autologous bone marrow or stem cell transplantation. Bone Marrow Transplant 12: 603–608. PMID: 7907905

17. Ballinger MN, Aronoff DM, McMillan TR, Cooke KR, Olkiewicz K, et al. (2006) Critical role of prostaglandin E2 overproduction in impaired pulmonary host response following bone marrow transplantation. J Immunol 177: 5499–5508. PMID: 17015736

18. Hubbard LL, Ballinger MN, Thomas PE, Wilke CA, Standiford TJ, et al. (2010) A role for IL-1 receptor-associated kinase-M in prostaglandin E2-induced immunosuppression post-bone marrow transplantation. J Immunol 184: 6299–6308. doi: 10.4049/jimmunol.0902828 PMID: 20439918

19. Domingo-Gonzalez R, Katz S, Serezani CH, Moore TA, Levine AM, et al. (2013) Prostaglandin E2-induced changes in alveolar macrophage scavenger receptor profiles differentially alter phagocytosis of Pseudomonas aeruginosa and Staphylococcus aureus post-bone marrow transplant. J Immunol 190: 5809–5817. doi: 10.4049/jimmunol.1203274 PMID: 23630358

20. Betz M, Fox BS (1991) Prostaglandin E2 inhibits production of Th1 lymphokines but not of Th2 lymphokines. J Immunol 146: 108–113. PMID: 1845802

21. Snijdewint FG, Kalinski P, Wierenga EA, Bos JD, Kapsenberg ML (1993) Prostaglandin E2 differentially modulates cytokine secretion profiles of human T helper lymphocytes. J Immunol 150: 5321–5329. PMID: 8390534

22. Aronoff DM, Canetti C, Peters-Golden M (2004) Prostaglandin E2 inhibits alveolar macrophage phagocytosis through an E-prostanoid 2 receptor-mediated increase in intracellular cyclic AMP. J Immunol 173: 559–565. PMID: 15210817

23. Serezani CH, Chung J, Ballinger MN, Moore BB, Aronoff DM, et al. (2007) Prostaglandin E2 suppresses bacterial killing in alveolar macrophages by inhibiting NADPH oxidase. Am J Respir Cell Mol Biol 37: 562–570. PMID: 17585108

24. Ginsberg HS, Moldawer LL, Sehgal PB, Redington M, Kilian PL, et al. (1991) A mouse model for investigating the molecular pathogenesis of adenovirus pneumonia. Proc Natl Acad Sci USA 88: 1651–1655. PMID: 1848005

25. Kajon AE, Gigliotti AP, Harrod KS (2003) Acute inflammatory response and remodeling of airway epithelium after subspecies B1 human adenovirus infection of the mouse lower respiratory tract. J Med Virol 71: 233–244. PMID: 12938198

26. Wigand R, Gelderblom H, Ozel M (1977) Biological and biophysical characteristics of mouse adenovirus, strain FL. Arch Virol 54: 131–142. PMID: 560839

27. Meissner JD, Hirsch GN, LaRue EA, Fulcher RA, Spindler KR (1997) Completion of the DNA sequence of mouse adenovirus type 1: sequence of E2B, L1, and L2 (18–51 map units). Virus Res 51: 53–64. PMID: 9381795

28. Ball AO, Williams ME, Spindler KR (1988) Identification of mouse adenovirus type 1 early region 1: DNA sequence and a conserved transactivating function. J Virol 62: 3947–3957. PMID: 3172335

29. Ball AO, Beard CW, Redick SD, Spindler KR (1989) Genome organization of mouse adenovirus type 1 early region 1: a novel transcription map. Virology 170: 523–536. PMID: 2543128

30. Ball AO, Beard CW, Villegas P, Spindler KR (1991) Early region 4 sequence and biological comparison of two isolates of mouse adenovirus type 1. Virology 180: 257–265. PMID: 1845825

31. Cauthen AN, Spindler KR (1996) Sequence of the mouse adenovirus type-1 DNA encoding the 100-kDa, 33-kDa and DNA-binding proteins. Gene 168: 183–187. PMID: 8654941

32. Kring SC, Spindler KR (1990) Sequence of mouse adenovirus type 1 DNA encoding the amino terminus of protein IVa2. Nucleic Acids Res 18: 4003. PMID: 2374728

33. Kring SC, Ball AO, Spindler KR (1992) Transcription mapping of mouse adenovirus type 1 early region 4. Virology 190: 248–255. PMID: 1388309

34. Anderson VE, Nguyen Y, Weinberg JB (2009) Effects of allergic airway disease on mouse adenovirus type 1 respiratory infection. Virology 391: 25–32. doi: 10.1016/j.virol.2009.06.009 PMID: 19564030

35. Weinberg JB, Stempfle GS, Wilkinson JE, Younger JG, Spindler KR (2005) Acute respiratory infection with mouse adenovirus type 1. Virology 340: 245–254. PMID: 16054189

36. Weinberg JB, Jensen DR, Gralinski LE, Lake AR, Stempfle GS, et al. (2007) Contributions of E1A to mouse adenovirus type 1 pathogenesis following intranasal inoculation. Virology 357: 54–67. PMID: 16962154

37. Procario MC, Levine RE, McCarthy MK, Kim E, Zhu L, et al. (2012) Susceptibility to acute mouse adenovirus type 1 respiratory infection and establishment of protective immunity in neonatal mice. J Virol 86: 4194–4203. doi: 10.1128/JVI.06967-11 PMID: 22345470

38. Nguyen Y, Procario MC, Ashley SL, O'Neal WK, Pickles RJ, et al. (2011) Limited effects of Muc1 deficiency on mouse adenovirus type 1 respiratory infection. Virus Res 160: 351–359. doi: 10.1016/j.virusres.2011.07.012 PMID: 21816184

39. Nguyen Y, McGuffie BA, Anderson VE, Weinberg JB (2008) Gammaherpesvirus modulation of mouse adenovirus type 1 pathogenesis. Virology 380: 182–190. doi: 10.1016/j.virol.2008.07.031 PMID: 18768196

40. McCarthy MK, Zhu L, Procario MC, Weinberg JB (2014) IL-17 contributes to neutrophil recruitment but not to control of viral replication during acute mouse adenovirus type 1 respiratory infection. Virology 456–457: 259–267. doi: 10.1016/j.virol.2014.04.008 PMID: 24889245

41. McCarthy MK, Levine RE, Procario MC, McDonnell PJ, Zhu L, et al. (2013) Prostaglandin E2 induction during mouse adenovirus type 1 respiratory infection regulates inflammatory mediator generation but does not affect viral pathogenesis. PLoS One 8: e77628. doi: 10.1371/journal.pone.0077628 PMID: 24147040

42. Trebino CE, Stock JL, Gibbons CP, Naiman BM, Wachtmann TS, et al. (2003) Impaired inflammatory and pain responses in mice lacking an inducible prostaglandin E synthase. Proc Natl Acad Sci U S A 100: 9044–9049. PMID: 12835414

43. Hubbard LL, Ballinger MN, Wilke CA, Moore BB (2008) Comparison of conditioning regimens for alveolar macrophage reconstitution and innate immune function post bone marrow transplant. Exp Lung Res 34: 263–275. doi: 10.1080/01902140802022518 PMID: 18465404

44. Cauthen AN, Welton AR, Spindler KR (2007) Construction of mouse adenovirus type 1 mutants. Methods Mol Med 130: 41–59. PMID: 17401163

45. Li J, Powell SR, Wang X (2011) Enhancement of proteasome function by PA28α overexpression protects against oxidative stress. FASEB J 25: 883–893. doi: 10.1096/fj.10-160895 PMID: 21098724

46. Chen Q, Liu JB, Horak KM, Zheng H, Kumarapeli AR, et al. (2005) Intrasarcoplasmic amyloidosis impairs proteolytic function of proteasomes in cardiomyocytes by compromising substrate uptake. Circ Res 97: 1018–1026. PMID: 16210548

47. Spandidos A, Wang X, Wang H, Seed B (2010) PrimerBank: a resource of human and mouse PCR primer pairs for gene expression detection and quantification. Nucleic Acids Res 38: D792–799. doi: 10.1093/nar/gkp1005 PMID: 19906719

48. Kapoor M, Kojima F, Qian M, Yang L, Crofford LJ (2006) Shunting of prostanoid biosynthesis in microsomal prostaglandin E synthase-1 null embryo fibroblasts: regulatory effects on inducible nitric oxide synthase expression and nitrite synthesis. FASEB J 20: 2387–2389. PMID: 17023389

49. Boulet L, Ouellet M, Bateman KP, Ethier D, Percival MD, et al. (2004) Deletion of microsomal prostaglandin E2 (PGE2) synthase-1 reduces inducible and basal PGE2 production and alters the gastric prostanoid profile. J Biol Chem 279: 23229–23237. PMID: 15016822

50. Duran-Struuck R, Dysko RC (2009) Principles of bone marrow transplantation (BMT): providing optimal veterinary and husbandry care to irradiated mice in BMT studies. J Am Assoc Lab Anim Sci 48: 11–22. PMID: 19245745

51. Gowdy KM, Martinu T, Nugent JL, Manzo ND, Zhang HL, et al. (2015) Impaired CD8(+) T cell immunity after allogeneic bone marrow transplantation leads to persistent and severe respiratory viral infection. Transpl Immunol 32: 51–60. doi: 10.1016/j.trim.2014.10.005 PMID: 25446809

52. Nagayama Y, Nakahara M, Shimamura M, Horie I, Arima K, et al. (2012) Prophylactic and therapeutic efficacies of a selective inhibitor of the immunoproteasome for Hashimoto's thyroiditis, but not for Graves' hyperthyroidism, in mice. Clin Exp Immunol 168: 268–273. doi: 10.1111/j.1365-2249.2012.04578.x PMID: 22519588

53. Coomes SM, Moore BB (2010) Pleiotropic effects of transforming growth factor-beta in hematopoietic stem-cell transplantation. Transplantation 90: 1139–1144. doi: 10.1097/TP.0b013e3181efd018 PMID: 20671593

54. Yao C, Sakata D, Esaki Y, Li Y, Matsuoka T, et al. (2009) Prostaglandin E2-EP4 signaling promotes immune inflammation through Th1 cell differentiation and Th17 cell expansion. Nat Med 15: 633–640. doi: 10.1038/nm.1968 PMID: 19465928

55. Nataraj C, Thomas DW, Tilley SL, Nguyen MT, Mannon R, et al. (2001) Receptors for prostaglandin E (2) that regulate cellular immune responses in the mouse. J Clin Invest 108: 1229–1235. PMID: 11602631

56. Coulombe F, Jaworska J, Verway M, Tzelepis F, Massoud A, et al. (2014) Targeted prostaglandin E2 inhibition enhances antiviral immunity through induction of type I interferon and apoptosis in macrophages. Immunity 40: 554–568. doi: 10.1016/j.immuni.2014.02.013 PMID: 24726877

57. Heemskerk B, Lankester AC, van Vreeswijk T, Beersma MF, Claas EC, et al. (2005) Immune reconstitution and clearance of human adenovirus viremia in pediatric stem-cell recipients. J Infect Dis 191: 520–530. PMID: 15655775

58. van Tol MJ, Claas EC, Heemskerk B, Veltrop-Duits LA, de Brouwer CS, et al. (2005) Adenovirus infection in children after allogeneic stem cell transplantation: diagnosis, treatment and immunity. Bone Marrow Transplant 35 Suppl 1: S73–76. PMID: 15812536

59. Zandvliet ML, Falkenburg JH, van Liempt E, Veltrop-Duits LA, Lankester AC, et al. (2010) Combined CD8+ and CD4+ adenovirus hexon-specific T cells associated with viral clearance after stem cell transplantation as treatment for adenovirus infection. Haematologica 95: 1943–1951. doi: 10.3324/haematol.2010.022947 PMID: 20562315

60. Rooney CM, Smith CA, Ng CY, Loftin SK, Sixbey JW, et al. (1998) Infusion of cytotoxic T cells for the prevention and treatment of Epstein-Barr virus-induced lymphoma in allogeneic transplant recipients. Blood 92: 1549–1555. PMID: 9716582

61. Heslop HE, Ng CY, Li C, Smith CA, Loftin SK, et al. (1996) Long-term restoration of immunity against Epstein-Barr virus infection by adoptive transfer of gene-modified virus-specific T lymphocytes. Nat Med 2: 551–555. PMID: 8616714

62. Rooney CM, Smith CA, Ng CY, Loftin S, Li C, et al. (1995) Use of gene-modified virus-specific T lymphocytes to control Epstein-Barr-virus-related lymphoproliferation. Lancet 345: 9–13. PMID: 7799740

63. Geyeregger R, Freimuller C, Stemberger J, Artwohl M, Witt V, et al. (2014) First-in-man clinical results with good manufacturing practice (GMP)-compliant polypeptide-expanded adenovirus-specific T cells after haploidentical hematopoietic stem cell transplantation. J Immunother 37: 245–249. doi: 10.1097/CJI.0000000000000034 PMID: 24714358

64. Leen AM, Christin A, Myers GD, Liu H, Cruz CR, et al. (2009) Cytotoxic T lymphocyte therapy with donor T cells prevents and treats adenovirus and Epstein-Barr virus infections after haploidentical and matched unrelated stem cell transplantation. Blood 114: 4283–4292. doi: 10.1182/blood-2009-07-232454 PMID: 19700662

65. Smith CA, Woodruff LS, Rooney C, Kitchingman GR (1998) Extensive cross-reactivity of adenovirus-specific cytotoxic T cells. Hum Gene Ther 9: 1419–1427. PMID: 9681413

66. Smith CA, Woodruff LS, Kitchingman GR, Rooney CM (1996) Adenovirus-pulsed dendritic cells stimulate human virus-specific T-cell responses in vitro. J Virol 70: 6733–6740. PMID: 8794310

67. Heemskerk B, Veltrop-Duits LA, van Vreeswijk T, ten Dam MM, Heidt S, et al. (2003) Extensive cross-reactivity of CD4+ adenovirus-specific T cells: implications for immunotherapy and gene therapy. J Virol 77: 6562–6566. PMID: 12743315

68. Feuchtinger T, Lang P, Hamprecht K, Schumm M, Greil J, et al. (2004) Isolation and expansion of human adenovirus-specific CD4+ and CD8+ T cells according to IFN-gamma secretion for adjuvant immunotherapy. Exp Hematol 32: 282–289. PMID: 15003314

69. Chakupurakal G, Onion D, Bonney S, Cobbold M, Mautner V, et al. (2013) HLA-peptide multimer selection of adenovirus-specific T cells for adoptive T-cell therapy. J Immunother 36: 423–431. doi: 10.1097/CJI.0b013e3182a8029e PMID: 23994889

70. Leen AM, Sili U, Savoldo B, Jewell AM, Piedra PA, et al. (2004) Fiber-modified adenoviruses generate subgroup cross-reactive, adenovirus-specific cytotoxic T lymphocytes for therapeutic applications. Blood 103: 1011–1019. PMID: 14525768

71. Basler M, Dajee M, Moll C, Groettrup M, Kirk CJ (2010) Prevention of experimental colitis by a selective inhibitor of the immunoproteasome. J Immunol 185: 634–641. doi: 10.4049/jimmunol.0903182 PMID: 20525886